 CMES, vol.94, no.2, pp.175-205, 2013

Using the Method of Fundamental Solutions for Obtaining Exponentially Convergent Helmholtz Eigensolutions

Chia-Cheng Tsai[1,2], **D. L. Young**[3]

Abstract: It is well known that the method of fundamental solutions (MFS) is a numerical method of exponential convergence. In this study, the exponential convergence of the MFS is demonstrated by obtaining the eigensolutions of the Helmholtz equation. In the solution procedure, the sought solution is approximated by a superposition of the Helmholtz fundamental solutions and a system matrix is resulted after imposing the boundary condition. A golden section determinant search method is applied to the matrix for finding exponentially convergent eigenfrequencies. In addition, the least-squares method of fundamental solutions is applied for solving the corresponding eigenfunctions. In the solution procedure, the sources of the MFS are located as far as possible and the precision saturation is avoided by using the multiple precision floating-point reliable (MPFR) library.

Keywords: exponential convergence, method of fundamental solutions, multiple precision floating-point reliable library, Helmholtz equation

1 Introduction

The method of fundamental solutions (MFS) was first proposed by Kupradze and Aleksidze (1964). Later, Mathon and Johnston (1977); Bogomolny (1985) established the mathematical fundamentals for the MFS. Then the MFS was successfully applied to the potential flow problems [Johnston and Fairweather (1984); Wu, Yang and Young (2011)], the biharmonic equation [Karageorghis and Fairweather (1987)], the Poisson equation [Golberg (1995)], the Stokes flow problems [Alves and Silvestre (2004); Tsai, Young, Fan and Chen (2006); Tsai, Young, Lo and Wong (2006); Young, Jane, Fan, Murugesan and Tsai (2006)], a cathodic protection problem [Santos, Santiago and Telles (2012)], the elastic problems [Tsai

[1] Corresponding author. Department of Marine Environmental Engineering, National Kaohsiung Marine University, Kaohsiung 811, Taiwan. E-mail: tsaichiacheng@mail.nkmu.edu.tw

[2] International Wave Dynamics Research Center, National Cheng Kung University, Tainan 701, Taiwan.

[3] Department of Civil Engineering, National Taiwan University, Taipei 106, Taiwan.

(2007); Tsai (2009)], the diffusion equations [Young, Tsai and Fan (2004); Young, Tsai, Murugesan, Fan and Chen (2004)] and some other time dependent problems [Gu, Young and Fan (2009); Lin, Gu and Young (2010)]. Comprehensive reviews of the MFS were given by Fairweather and Karageorghis (1998) and Golberg and Chen (1999).

The MFS has also been applied to problems governed by the Helmholtz equation. Kondapalli, Shippy and Fairweather (1992) were among the first to apply the MFS for the Helmholtz equation in the analysis of acoustic scattering. Then, Karageorghis (2001) applied the MFS to obtain eigenvalues of the Helmholtz equation in two-dimensional simply-connected domains, and Chen, Chen and Lee (2005) solved eigenvalues in two-dimensional multiply-connected domains. Tsai, Young, Chen and Fan (2006) summarized the MFS applications for eigenvalues in two- and three-dimensional domains with and without interior holes. In most of these works [Karageorghis (2001); Chen, Young, Tsai and Murugesan (2005); Tsai, Young, Chen and Fan (2006)] the MFS in conjunction with the direct determinant search method was applied to obtain the eigenvalues. Furthermore, it was found that the eigenvalues obtained by the MFS are highly accurate with very few nodes. The ability of determination of the eigenvalues by MFS is unquestionable although its exponential convergence is not yet shown before.

For the Helmholtz eigenfunctions, the singular value decomposition (SVD) has been maturely applied to obtain the contours of acoustical modes after the eigenvalues are solved in the applications of boundary integral equation method (BIEM) [Chen, Huang and Wong (2000)]. However, it is found that that the ill-conditionings of MFS [Christiansen and Meister (1981)] and the singularities of eigenfunctions interacted and made the mode shapes sensitive with respect to the locations of source points when the MFS with SVD was utilized [Tsai, Young, Chiu and Fan (2009)]. On the other hand, Chen, Chen and Chyuan (1999) applied the dual BEM to obtain the eigenfunctions of a square cavity by specifying an additional normalization condition. It results in the least-squares MFS [Smyrlis and Karageorghis (2004); Tsai, Young, Chiu and Fan (2009)] when the prescribed idea is applied to the MFS. In this study, the exponential convergence of the eigenfunctions obtained by the least-squares MFS will also be demonstrated.

In order to improve the accuracy of the solutions obtained by the MFS, the sources should be located far away from the boundary which however results in severe ill-conditioning and instability [Mathon and Johnston (1977); Bogomolny (1985); Tsai, Lin, Young and Aturi (2006); Tsai and Lin (2013)]. Therefore Smyrlis, Karageorghis and Georgiou (2001) studied the issue and normalized the fundamental solution to reduce the conditioning of the considered problems. In addition, Ramachandran (2002) and Chen, Cho and Golberg (2006) used the SVD to mitigate

the ill-conditioning. Also, Wei et al. Wei, Hon and Ling (2007) used various regularization techniques to study the MFS solution of Cauchy problems. On the other hand, Tsai and Lin (2013) put the source as far as possible and used the multiple-precision computing for obtaining exponentially convergent solutions of Laplace equation. In study, the idea is extended to obtain exponentially convergent Helmholtz eigenvalues and eigenfunctions.

Although the IEEE 80-bit extended floating-point arithmetic, whose machine epsilon is $2^{-63} \cong 10^{-19}$, is sufficiently accurate for most scientific applications, there are still certain scientific computing applications require a higher level of numeric precision. Several software tools exist for multiple-precision floating-point arithmetic. The commercial products Mathematica [Wolfram (1996)] and Maple [Char, Geddes, Gonnet, Leong, Monagan and Watt (1991)] are the most common software provide multiple-precision floating-point arithmetic. However, the codes in these products cannot be easily communicated with other existing scientific programs written in high-level programming languages. For high-precision arithmetic software written in high-level programming languages, Brent (1978) developed a FORTRAN multiple-precision arithmetic package. On the other hand, Bailey, Yozo, Li and Thompson (2002) implemented the ARPREC which is able to perform arithmetic with an arbitrarily high level of precision and has high-level language interfaces for both C++ and FORTRAN. Alternatively, Batut, Belabas, Bernardi, Cohen and Oliver (2000) and Haible and Kreckel (2005) produced the PARI/GP and the CLN, respectively. In addition, Granlund (2004) coded the GMP which has both the multiple-precision float-point numbers and big integers. However, these packages do not provide clear semantics and correct rounding as defined in IEEE 754. The multiple precision floating-point reliable (MPFR) library was thus developed by Hanrot, Lefevre, Pelissier and Zimmermann (2005). The MPFR library provides correct rounding for all the operations and mathematical functions it implements. A comprehensive review of the MPFR library can be found in the literature [Fousse, Hanrot, Lefevre, Pelissier and Zimmermann (2007)]. And a recent introduction of these multiple-precision packages and their applications are drawn by Bailey and Borwein (2008).

In this paper, the exponential convergence of the Helmholtz eigenvalues and eigenfunctions are demonstrated by a golden section determinant search method and least-squares MFS, respectively. Overall, this paper is organized as follows: the MFS formulation for eigenvalues and the least-squares MFS formulation for eigenfunctions are reviewed in Section 2 and 3 respectively. In Section 4, the golden section determinant search method is introduced. Some numerical results are presented in Section 5 and conclusions are drawn in Section 6.

2 MFS formulation for eigenvalues

Consider an eigenproblem governed by the Helmholtz equation as

$$\left(\nabla^2 + k^2\right) u(\mathbf{x}) = 0 \quad \text{for} \quad \mathbf{x} \in \Omega \tag{1}$$

with boundary conditions

$$u(\mathbf{x}) = 0 \quad \text{for} \quad \mathbf{x} \in \Gamma^D \tag{2}$$

and

$$\frac{\partial u}{\partial \mathbf{n}_\mathbf{x}}(\mathbf{x}) = 0 \quad \text{for} \quad \mathbf{x} \in \Gamma^N \tag{3}$$

where ∇^2 is the Laplacian operator, k is the wavenumber, Ω is the domain of interest, $\Gamma = \Gamma^D + \Gamma^N$ is the boundary of Ω, and $\mathbf{n}_\mathbf{x}$ is the outward unit normal vector of Γ (Figure 1(a)). The fundamental solution of the Helmholtz equation (1) is defined by

$$-(\nabla^2 + k^2) G_k(\mathbf{x}, \mathbf{s}) = \delta(\mathbf{x} - \mathbf{s}) \tag{4}$$

where $\mathbf{x}$ are the coordinates of field points and $\mathbf{s}$ are the coordinates of source points. Then, the fundamental solutions can be obtained as

$$G_k(\mathbf{x}, \mathbf{s}) = \frac{\mathbf{i}}{4} H_0^{(1)}(k|\mathbf{x} - \mathbf{s}|) \tag{5}$$

where $\mathbf{i}$ is the complex unit and $H_0^{(1)}()$ is the first kind Hankel function of order zero. In the spirit of the MFS, the solution can be approximated by

$$u(\mathbf{x}) \cong \tilde{u}(\mathbf{x}) = \sum_{j=1}^{N} \alpha_j G_k(\mathbf{x}, \mathbf{s}_j) \tag{6}$$

where α_j is the intensity of the source point at $\mathbf{s}_j$, and N is the number of source points as depicted in Figure 1(b). In the present work, we uniformly distribute boundary field points and locate the source points by using the following formula:

$$\mathbf{s}_i = \mathbf{x}_c + \beta \times (\mathbf{x}_i - \mathbf{x}_c) \tag{7}$$

where $\mathbf{x}_c$ are the spatial coordinates of the domain center and b is a source parameter as depicted in Figure 1(b). If boundary conditions (2) and (3) are collocated on N

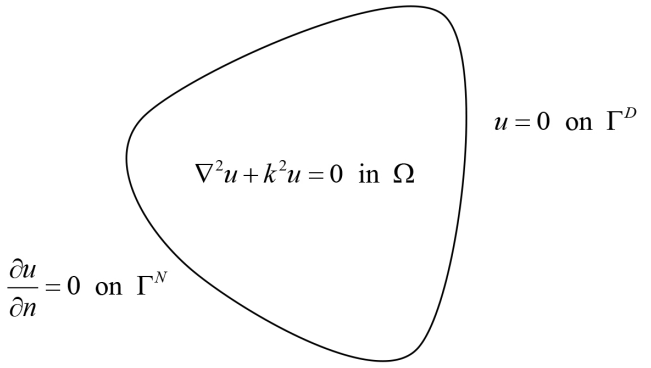

(a)

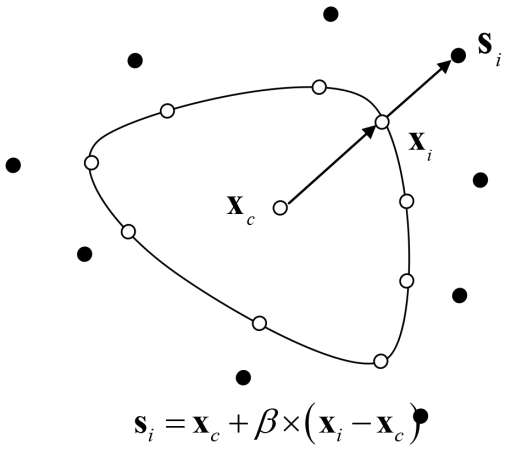

(b)

Figure 1: Schematic diagram of (a) Helmholtz problem and (b) MFS source configuration.

points, it results in a $N \times N$ linear system as

$$\mathbf{A}_k(\mathbf{x}_1, \mathbf{x}_2, ..., \mathbf{x}_N; \mathbf{s}_1, \mathbf{s}_1, ..., \mathbf{s}_N) \begin{bmatrix} \alpha_1 \\ \alpha_2 \\ \vdots \\ \vdots \\ \alpha_N \end{bmatrix} = \begin{bmatrix} 0 \\ 0 \\ \vdots \\ \vdots \\ 0 \end{bmatrix} \tag{8}$$

with

$$\mathbf{A}_k\left(\mathbf{x}_1,\mathbf{x}_2,...,\mathbf{x}_N;\mathbf{s}_1,\mathbf{s}_1,...,\mathbf{s}_N\right)=\begin{bmatrix} A_k\left(\mathbf{x}_1,\mathbf{s}_1\right) & A_k\left(\mathbf{x}_1,\mathbf{s}_2\right) & \cdots & \cdots & A_k\left(\mathbf{x}_1,\mathbf{s}_N\right) \\ A_k\left(\mathbf{x}_2,\mathbf{s}_1\right) & A_k\left(\mathbf{x}_2,\mathbf{s}_2\right) & \cdots & \cdots & A_k\left(\mathbf{x}_2,\mathbf{s}_N\right) \\ \vdots & \vdots & \ddots & \ddots & \vdots \\ \vdots & \vdots & \ddots & \ddots & \vdots \\ A_k\left(\mathbf{x}_N,\mathbf{s}_1\right) & A_k\left(\mathbf{x}_N,\mathbf{s}_2\right) & \cdots & \cdots & A_k\left(\mathbf{x}_N,\mathbf{s}_N\right) \end{bmatrix} \tag{9}$$

where $A_k\left(\mathbf{x}_i,\mathbf{s}_j\right)=G_k\left(\mathbf{x}_i,\mathbf{s}_j\right)$ if $\mathbf{x}_i\in\Gamma^D$ and $A_k\left(\mathbf{x}_i,\mathbf{s}_j\right)=\frac{\partial G_k}{\partial \mathbf{n}_\mathbf{x}}\left(\mathbf{x}_i,\mathbf{s}_j\right)$ if $\mathbf{x}_i\in\Gamma^N$. Equation (8) is a nonlinear eigenproblem in which we are searching for eigenvalues $0<k_1<k_2<k_3<\cdots$ such that the equation (8) has nontrivial solutions or equivalently the determinant of the system matrix in equation (8) is zero. A numerical method for obtaining exponentially convergent eigenvalues will be introduced in the next section.

If there are interior holes in the computational domain, a straight application of the single-layer (6) MFS formulation will result in spurious eigenvalues. Therefore, the MFS approximation (6) should be replaced by a mixed-layers expression as

$$u\left(\mathbf{x}\right)\cong\tilde{u}\left(\mathbf{x}\right)=\sum_{j=1}^{N_1}\alpha_{1j}G_k\left(\mathbf{x},\mathbf{s}_{1j}\right)+\sum_{j=1}^{N_2}\alpha_{2j}\left(G_k\left(\mathbf{x},\mathbf{s}_{2j}\right)+\mathbf{i}k\frac{\partial G_k}{\partial \mathbf{n}_s}\left(\mathbf{x},\mathbf{s}_{2j}\right)\right) \tag{10}$$

where α_{1j} is the intensity of the exterior source point at $\mathbf{s}_{1j}$, α_{2j} is the intensity of the interior source point at $\mathbf{s}_{2j}$, and $\mathbf{n}_s$ the inward unit normal vector of a fictitious curve on which the interior source points are located. Moreover, N_1 and N_2 are the corresponding numbers of source points as depicted in Figure 2. More details of the mixed-layers MFS can be found in the literature [Tsai, Young, Chen and Fan (2006)].

3 Least-squares MFS formulation for eigenfunctions

After the eigenvalues $0<k_1<k_2<k_3<\cdots$ are found, we are ready to find the corresponding eigenfunctions $u_1\left(\mathbf{x}\right),u_2\left(\mathbf{x}\right),u_3\left(\mathbf{x}\right),\ldots$. Considering $k=k'$ being an eigenvalue with multiplicity equal to one and $\mathbf{y}\in\Gamma$ being a specific boundary point, the eigenfunction can be uniquely determined by

$$\left(\nabla^2+k'^2\right)u\left(\mathbf{x}\right)=0 \text{ for } \mathbf{x}\in\Omega \tag{11}$$

together with the boundary condition (2)$\sim$(3) and a normalization condition

$$\frac{\partial u}{\partial \mathbf{n}_\mathbf{x}}\left(\mathbf{y}\right)=1 \text{ for } \mathbf{y}\in\Gamma^D \tag{12}$$

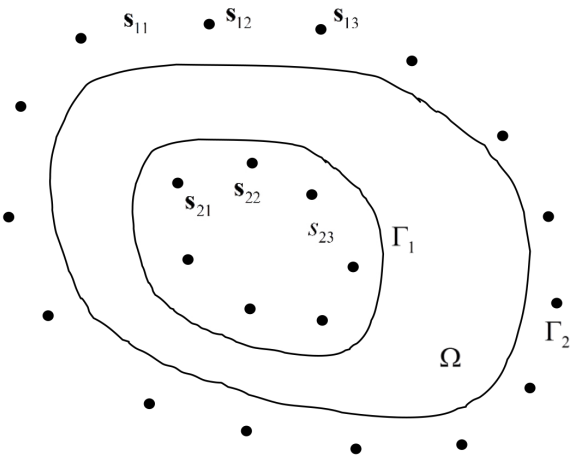

Figure 2: Schematic diagram of MFS source configuration for problem with a interior hole.

or

$$u(\mathbf{y}) = 1 \quad \text{for} \quad \mathbf{y} \in \Gamma^{\mathrm{N}} \tag{13}$$

To ensure the system defined by Eqs. (2), (3), (11)$\sim$(13) has a unique solution, we should also assume that the augmented boundary point $\mathbf{y}$ is away from the nodal curves of the sought eigenfunction. In practical implementation, this condition can always be fulfilled by arranging the location of $\mathbf{y}$. More details can be found in the literature [Tsai, Young, Chiu and Fan (2009)].

By the MFS approximation (6), the prescribed system can be numerically converted to the least-squares solution of the following system of linear equations:

$$\mathbf{B}_{k'}(\mathbf{x}_1, \mathbf{x}_2, ..., \mathbf{x}_N, \mathbf{y}; \mathbf{s}_1, \mathbf{s}_1, ..., \mathbf{s}_N) \begin{bmatrix} \alpha_1 \\ \alpha_2 \\ \vdots \\ \vdots \\ \alpha_N \end{bmatrix} = \begin{bmatrix} 0 \\ 0 \\ \vdots \\ \vdots \\ 0 \\ 1 \end{bmatrix} \tag{14}$$

with

$$\mathbf{B}_{k'}(\mathbf{x}_1, \mathbf{x}_2, ..., \mathbf{x}_N, \mathbf{y}; \mathbf{s}_1, \mathbf{s}_1, ..., \mathbf{s}_N) = \begin{bmatrix} \mathbf{A}_{k'}(\mathbf{x}_1, \mathbf{x}_2, ..., \mathbf{x}_N; \mathbf{s}_1, \mathbf{s}_1, ..., \mathbf{s}_N) \\ B_{k'}(\mathbf{y}, \mathbf{s}_1) B_{k'}(\mathbf{y}, \mathbf{s}_2) \cdots B_{k'}(\mathbf{y}, \mathbf{s}_N) \end{bmatrix} \tag{15}$$

where $B_{k'}(\mathbf{y},\mathbf{s}_j)=\frac{\partial G_{k'}}{\partial \mathbf{n}_x}(\mathbf{y},\mathbf{s}_j)$ if $\mathbf{y}\in\Gamma^D$ and similarly for $\mathbf{y}\in\Gamma^N$. Clearly, Eq. (14) admits a least-squares solution as

$$\mathbf{B}^T\mathbf{B}\begin{bmatrix}\alpha_1\\ \alpha_2\\ \vdots\\ \vdots\\ \alpha_N\end{bmatrix}=\mathbf{B}^T\begin{bmatrix}0\\ 0\\ \vdots\\ \vdots\\ 0\\ 1\end{bmatrix}, \tag{16}$$

which can be formally solved by the LU decomposition. After the intensities α_j's are obtained, the corresponding eigenfunction can be approximated by using Eq. (6).

For cases with multiplicity greater than one, more augmented boundary points should be considered. More details can be found in the literature [Tsai, Young, Chiu and Fan (2009)].

4 Determinant search method

If it is desired to find the eigenvalues, it seems straightforward to calculate the determinant

$$\Delta(k)=\det\{\mathbf{A}_k(\mathbf{x}_1,\mathbf{x}_2,...,\mathbf{x}_N;\mathbf{s}_1,\mathbf{s}_1,...,\mathbf{s}_N)\} \tag{17}$$

at uniformly distributed points $\delta k, 2\delta k,....$ Then the eigenvalues are approximated by the k values associated to local minima of $\Delta(k)$, which will be demonstrated in the next section. However, the prescribed uniform determinant search method (UDSM) cannot be applied for obtaining exponentially convergent eigenvalues since it is time consuming.

Alternatively, it is well-known that the golden section search [William and Teukolsky (1988)] is a technique for finding the minimum of a unimodal function by successively narrowing the range of values inside which the minimum is known to exist. Here, a unimodal function is defined in an interval such that it has a unique minimum inside the interval and monotonically increases away from the minimum. As a nature consequence, we may perform a golden section determinant search method (GSDSM) for obtaining exponentially convergent eigenvalues.

In summary, a numerical method for obtaining an exponentially convergent eigenvalue is listed as follows:

Step 1: Apply the UDSM for finding a unimodal interval $a\le k\le b$ with $b-a=\delta k$ such that the determinant function $\Delta(k)$ has a local minimum at $k=a$ (or $k=b$) and $\Delta(b)<\Delta(a-\delta k)$ (or $\Delta(a)<\Delta(b+\delta k)$).

Step 2: Set c such that $\frac{c-a}{b-c} = \alpha$ where $\alpha = \frac{1+\sqrt{5}}{2}$ is the golden ratio.

Step 3: Check $c-a > b-c$ or $c-a < b-c$.

For $c-a > b-c$:

Step 4: Set d such that $\frac{d-a}{c-d} = \alpha$

Step 5: Set $a = d$ if $\Delta(c) < \Delta(d)$ and set $b = c$ and $c = d$ if $\Delta(d) < \Delta(c)$.

For $c-a < b-c$:

Step 4: Set d such that $\frac{b-d}{d-c} = \alpha$

Step 5: Set $b = d$ if $\Delta(c) < \Delta(d)$ and set $a = c$ and $c = d$ if $\Delta(d) < \Delta(c)$.

Step 6: Repeat Steps 3$\sim$5 until $b-a < \varepsilon$. Then the solution is equal to c.

In Step 1, $\delta k = 0.01$ is usually sufficient to find a unimodal interval according to our numerical experiments. If δk is too large, one may miss certain eigenvalues. And in Step 6, ε is a prescribed threshold which is usually set to be the machine epsilon of the working precision.

5 Numerical results

Now, we are in a position to show the exponential convergences of the MFS. Three numerical examples will be considered. One of them is a doubly-connected problem.

Example 1:

First of all, we solve the Helmholtz problem (1) and (2) in $\Omega = \{(x,y) | -\frac{\pi}{4} \le x \le \frac{\pi}{4}$ and $-\frac{1}{2} \le y \le \frac{1}{2}\}$ with Γ^D (Dirichlet boundary) being the whole boundary of Ω and $\mathbf{x} = (x,y)$. Obviously, we have the analytical eigenvalues given as

$$k' = \sqrt{(2m)^2 + (\pi n)^2} \tag{18}$$

and the corresponding eigenfunctions are

$$u = C \sin(2mx) \sin(\pi n y) \tag{19}$$

with C being a normalization constant that can be uniquely determined by Eq. (12). In Eqs. (18) and (19), m and n are positive integers.

Figure 3 gives the result of UDSM ($\delta k = 0.01$ and $\beta = 1.5$) for different numbers of nodes, which are basically consistent except for the cases of high frequencies, which require higher resolutions. In the figure, every cusp admits an eigenvalue and thus provides a unimodal interval for the GSDSM. Considering $m = n = 1$, the UDSM ($N = 40$ and $\beta = 1.5$) is performed between 3.70 and 3.74 for different δk

in Figure 4(a). For $\delta k = 0.0001$, it requires 401 iterations while only 16 iterations are required for the GSDSM to obtain an eigenvalue with similar accuracy. Then we push the sources farther ($\beta = 4$), we can obtain an eigenvalue with accuracy up to 1.86×10^{-11} with only 43 iterations by the GSDSM as shown in Figure 4(b) and Table I.

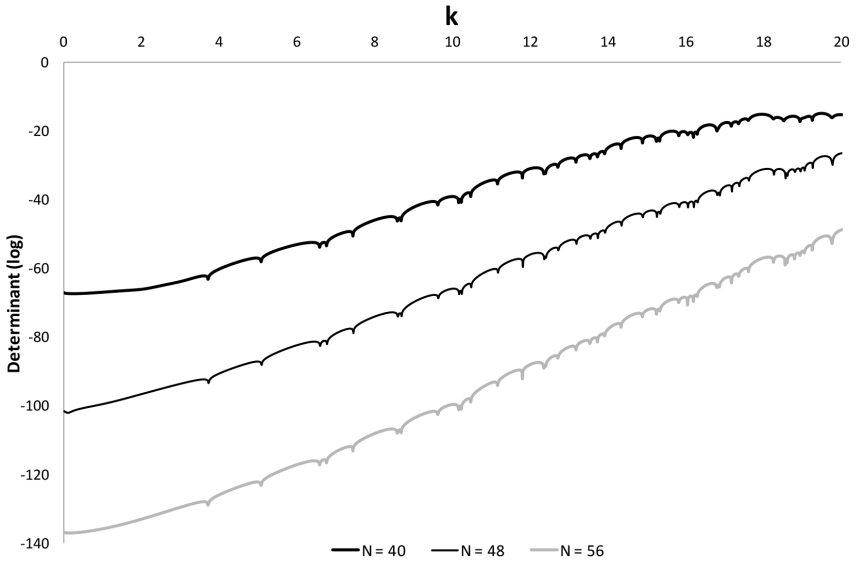

Figure 3: Results of UDSM of Example 1.

Table 1: Accuracy, numbers of iteration, and computing time (shadow for predicted time) for mode (1,1) eigenvalues in Example 1.

Method	Iteration	Accuracy	Time (sec)	Time (days)
UDSM	5	1.00E-02	0.054	
	41	1.00E-03	0.530	
	401	1.00E-04	5.454	
	2.2E+09	1.86E-11	2.31E+07	267
GSDSM	43	1.86E-11	0.462	

For $m = n = 1$ or equivalently mode (1,1), Figure 5(a) describes the relation between the accuracy and source parameter for different numbers of nodes. Basically, the cases of farther sources give better accuracy. For $N = 40$, the accuracy is

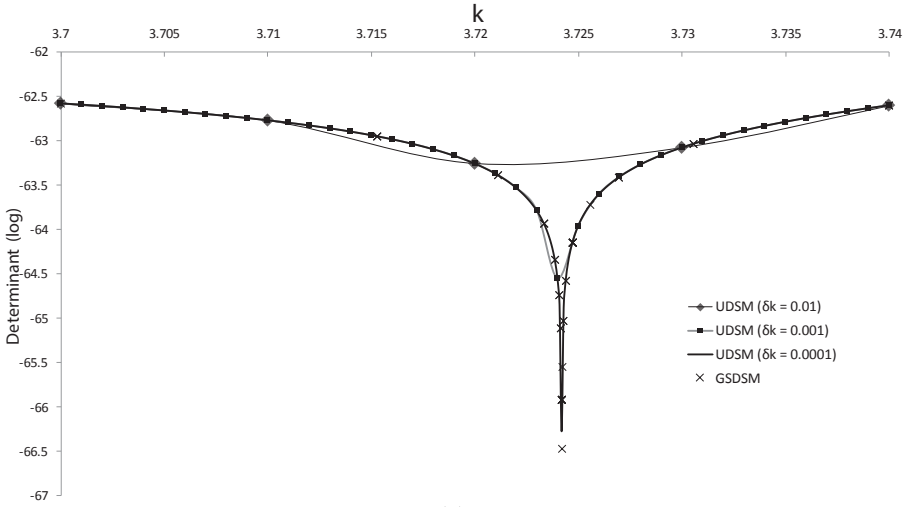

(a)

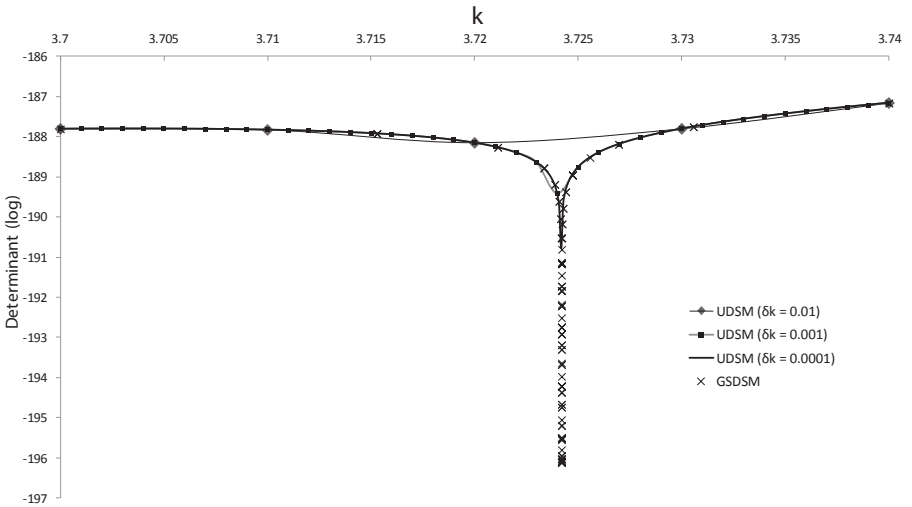

(b)

Figure 4: Comparison between UDSM and GSDSM for different source location (a) $\beta = 1.5$ and (b) $\beta = 4$.

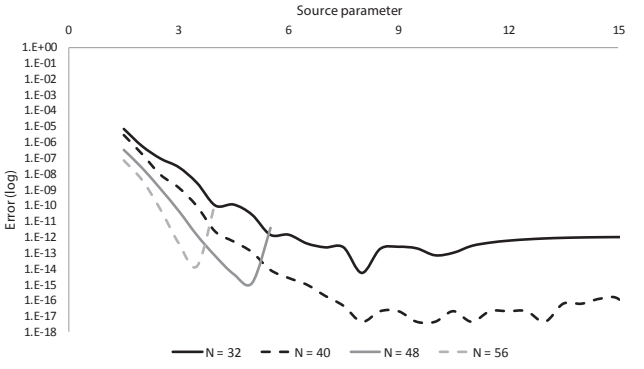

(a)

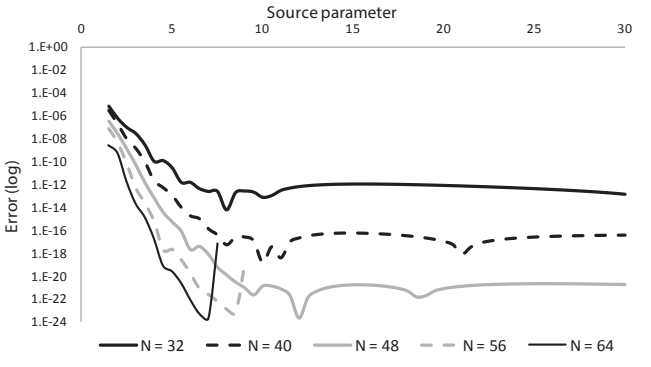

(b)

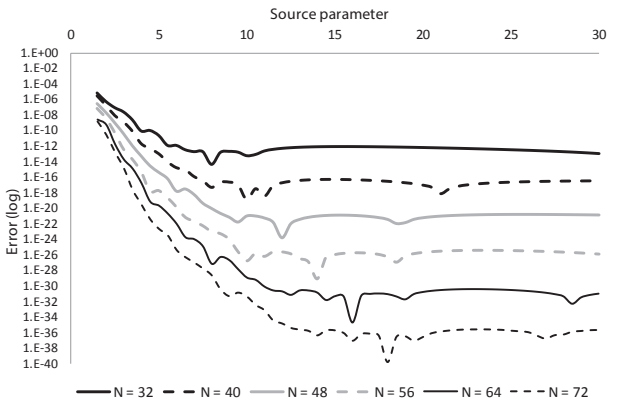

(c)

Figure 5: Relation between accuracy and source parameter for (a) IEEE extended precision, (b) MPFR ($p = 100$) and (b) MPFR ($p = 150$) for mode (1,1) eigenvalue in Example 1.

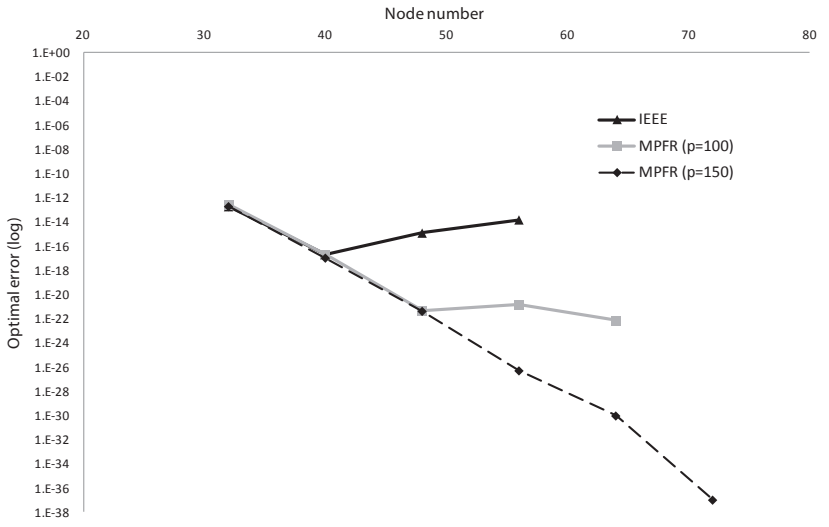

Figure 6: The exponential convergence of mode (1,1) eigenvalue in Example 1.

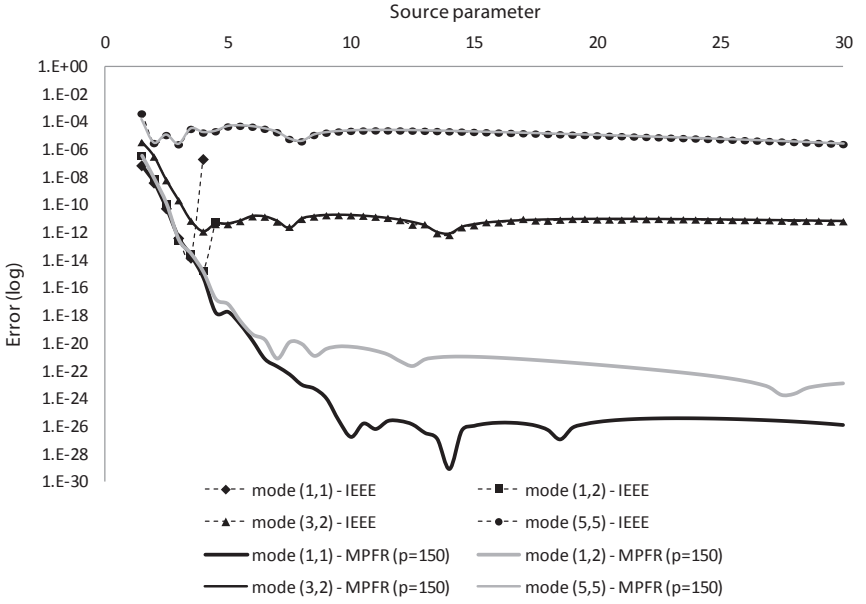

Figure 7: Relation between accuracy and source parameter for different modes of Example 1.

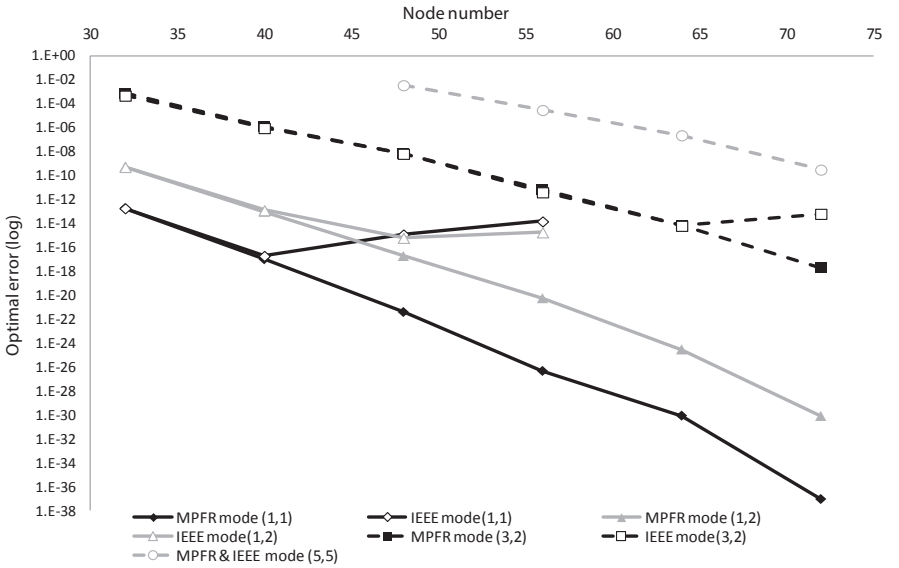

Figure 8: The exponential convergences of eigenvalues for different modes of Example 1.

4.12×10^{-18} by simply put the sources to a nine times bigger rectangle. This accuracy is very close to the machine epsilon of the IEEE extended precision. However for $N = 48$ and $N = 58$, they are in precision saturation such that increasing resolution cannot improve the accuracy without increasing precision. To further improve the accuracy, the working precision is changed from the IEEE extended precision to the MPFR with different precisions (p). The results are demonstrated in Figure 5(b) and 5(c) for $p = 100$ and $p = 150$ respectively. Using the GSDSM with 72 nodes, we can obtain a numerical eigenvalue with accuracy up to 9.11×10^{-38} by simply put the sources to a sixteen times bigger rectangle. Then, the exponential convergence is demonstrated in Figure 6, which indicates that the logarithmic error is proportional to the node numbers.

Then we apply the GSDSM to the cases of higher frequencies. Figure 7 shows the relation between the accuracy and source parameter for different modes with $N = 56$. For mode (1,1) and mode (1,2), they are in the IEEE extended precision saturation and thus increasing the working precision to MPFR ($p = 150$) does significantly improve the numerical accuracy. However, mode (3,2) and mode (5,5) are not in precision saturation and therefore increasing the working precision provides no improvement. Figure 8 demonstrates the exponential convergences of the obtained numerical eigenvalues of these modes. In the figure, it can be observed

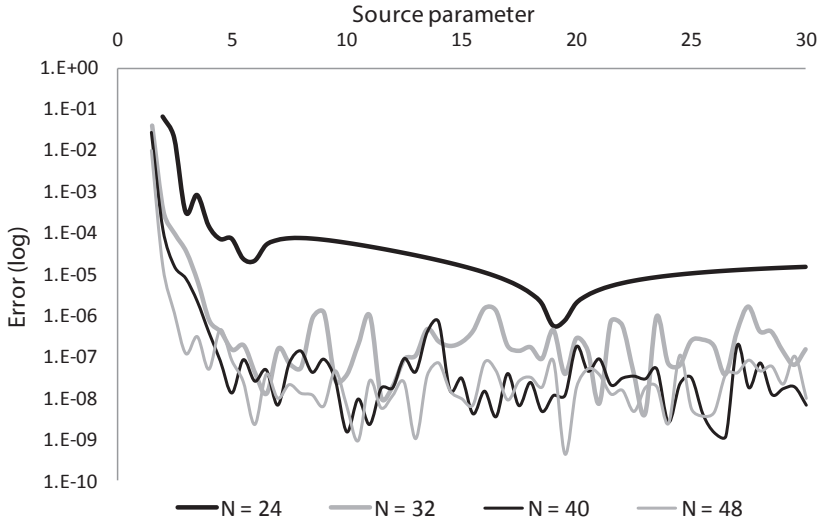

(a)

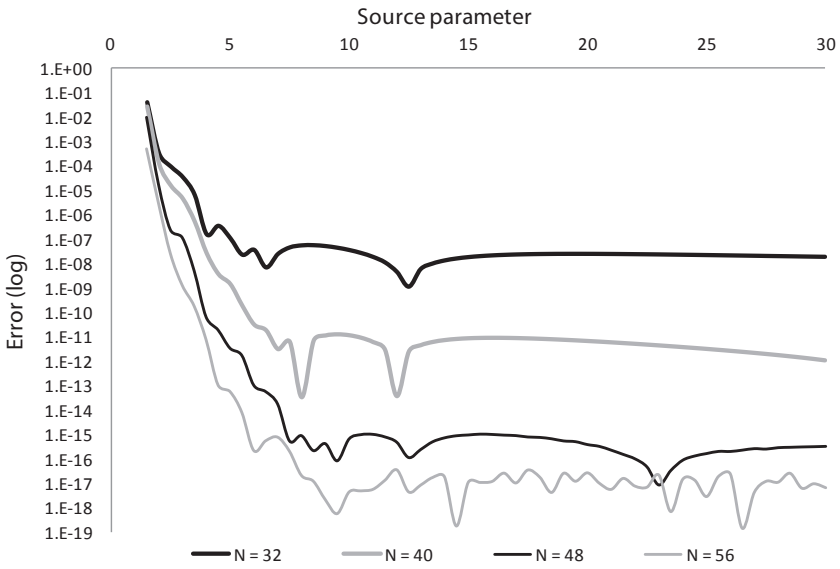

(b)

Figure 9: Relation between accuracy and source parameter for (a) IEEE extended precision and (b) MPFR ($p = 150$) for mode (1,1) eigenfunction in Example 1.

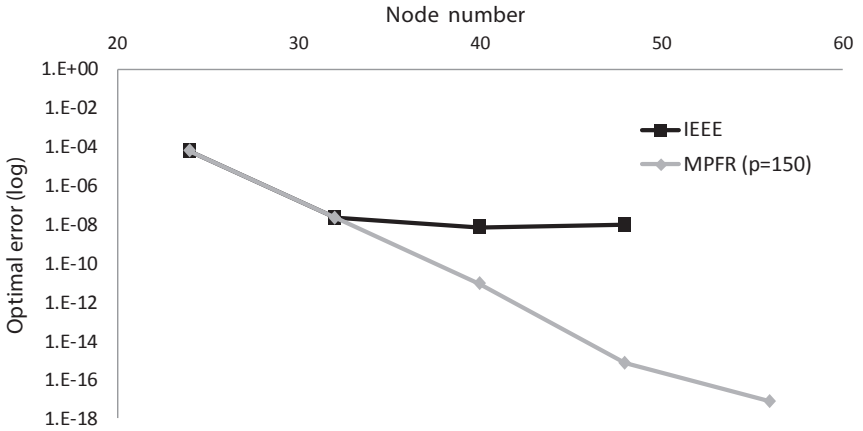

Figure 10: The exponential convergence of mode (1,1) eigenfunction in Example 1.

that higher resolutions are required for higher frequencies to achieve the same accuracy while their convergence rates (slopes) are basically similar. Furthermore, the IEEE precision saturations are significant for mode (1,1), mode (1,2) and mode (3,2).

Lastly, we consider the numerical eigenfunction of the mode (1,1) obtained by the least-squares MFS. Figure 9 gives the relation between the accuracy and source parameter. Considering the IEEE extended precision, precision saturations occur for the cases of $N = 24$, $N = 32$ and $N = 40$ as depicted in Figure 9(a). By changing the working precision from the IEEE extended precision to the MPFR ($p = 150$), the numerical accuracy does improve significantly as shown in Figure 9(b). In Figure 10, the exponential convergence is also demonstrated. Comparing the GSDSM solution of eigenvalues and the least-squares MFS solution of eigenfunctions, the later one is much more ill-conditioned in the sense that its saturated accuracy is much worse compared to the former one as shown in Table II.

Table 2: Saturated accuracy of eigenvalue and eigenfunctions of Example 1.

N	Eigenfunction	Eigenvalue
32	2.02E-08	-
40	6.80E-09	1.93E-17
48	9.00E-09	1.20E-15

Example 2:

Then, we consider the solution of Helmholtz equation (1) in an ellipse with major semi-axis $\bar{a} = 2$ and minor semi-axis $\bar{b} = 1$. Dirichlet boundary condition (2) is imposed on the ellipse. In this example, the elliptic coordinates (ξ, η) are defined as

$$\begin{cases} x = \bar{c}\cosh\xi\cos\eta \\ y = \bar{c}\sinh\xi\sin\eta \end{cases} \tag{20}$$

where $\bar{c} = \sqrt{\bar{a}^2 - \bar{b}^2}$ is the semi-focal distance, the radial coordinate ξ is a non-negative real number and the angular coordinate η is defined between 0 and 2π. According to the Mathieu's elliptic function theory [Frank, Daniel, Ronald and Charles (2010)], we have the even eigenvalues k' given as the positive roots of

$$Ce_m\left(q, \operatorname{acosh}\left(\frac{\bar{a}}{\bar{c}}\right)\right) = 0 \tag{21}$$

and the corresponding eigenfunctions are

$$u = C\{Ce_m(q,\xi)\, ce_m(q,\eta)\} \tag{22}$$

with q defined as $\frac{k'^2\bar{c}^2}{4}$ and C being a normalization constant that can be uniquely determined by Eq. (12). In Eqs. (20) and (22), ce_m and Ce_m are respectively the mth-order even Mathieu function and modified Mathieu function with m being a nonnegative integer.

Similarly, we have the odd eigenvalues k' given as the positive roots of

$$Se_m\left(q, \operatorname{acosh}\left(\frac{\bar{a}}{\bar{c}}\right)\right) = 0 \tag{23}$$

and the corresponding eigenfunctions are

$$u = C\{Se_m(q,\xi)\, se_m(q,\eta)\} \tag{24}$$

with se_m and Se_m being respectively the mth-order odd Mathieu function and modified Mathieu function with m being a positive integer.

The UDSM ($\delta k = 0.01$ and $\beta = 1.5$) is first performed to find a unimodal interval for each eigenvalue as shown in Figure 11. Then, the GSDSM is applied for finding exponentially convergent eigenvalues. Figure 12 gives the relation between the accuracy and source parameter for the smallest even eigenvalue of Eq. (21) with $m = 0$, which is denoted as mode (e,0,1). In the figure, it is found that the MFS

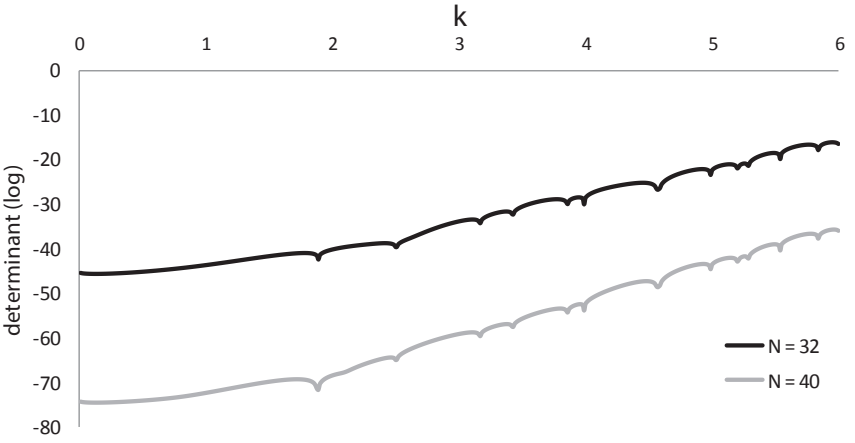

Figure 11: Results of UDSM of Example 2.

solution of Hankel functions (6) can approximate the even Mathieu function highly accurately. Using the GSDSM with 48 nodes, we can obtain a numerical eigenvalue with accuracy up to 2.99×10^{-37} by simply put the sources to a eleven times bigger ellipse. In Figure 13, similar results can also be observed for the case of the smallest odd eigenvalue of Eq. (23) with $m = 1$, which is denoted as mode (o,1,1). Figure 14 gives the exponential convergences of the two modes. In the figure, it can be observed that higher resolutions are required for mode (o,1,1), which is of a higher frequency. In addition, the IEEE precision saturations are significant for both modes.

Then, we consider the numerical eigenfunctions of the mode (e,0,1) obtained by the least-squares MFS. Figure 15 gives the relation between the accuracy and source parameter. By changing the working precision from the IEEE extended precision to the MPFR ($p = 150$), the numerical accuracy improves significantly as shown in Figure 15(b). Also, the exponential convergence of least-squares MFS solution is given in Figure 16. Similar to the previous example, the least-squares MFS solution of eigenfunctions is more ill-conditioned compared with the GSDSM solution of eigenvalues.

Overall, we demonstrate that the MFS solutions of Hankel functions (6) can approximate the Mathieu functions with exponential convergence. Before closing the discussion of this example, we should also mention that the MPFR Mathieu functions are extended from the double precision Mathieu functions [Alhargan (2000a); Alhargan (2000b)].

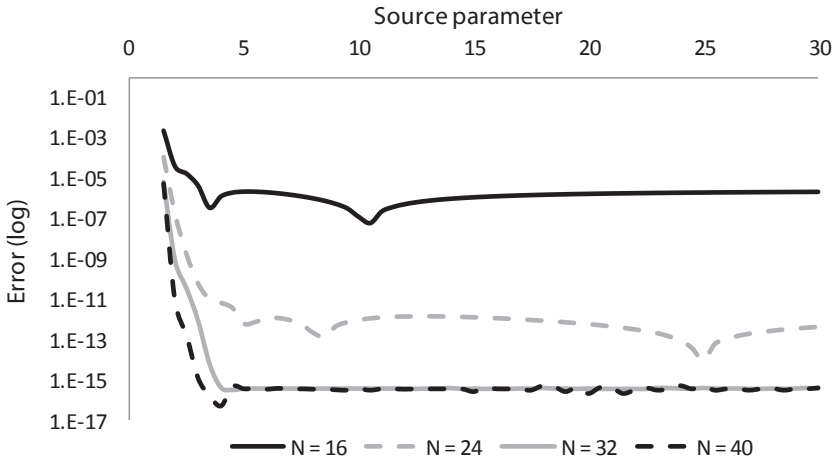

(a)

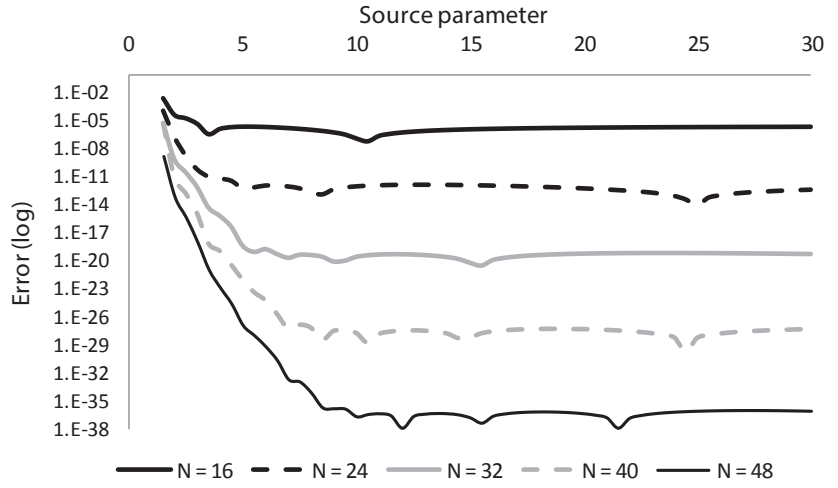

(b)

Figure 12: Relation between accuracy and source parameter for (a) IEEE extended precision and (b) MPFR ($p = 150$) for mode (e,0,1) eigenvalue in Example 2.

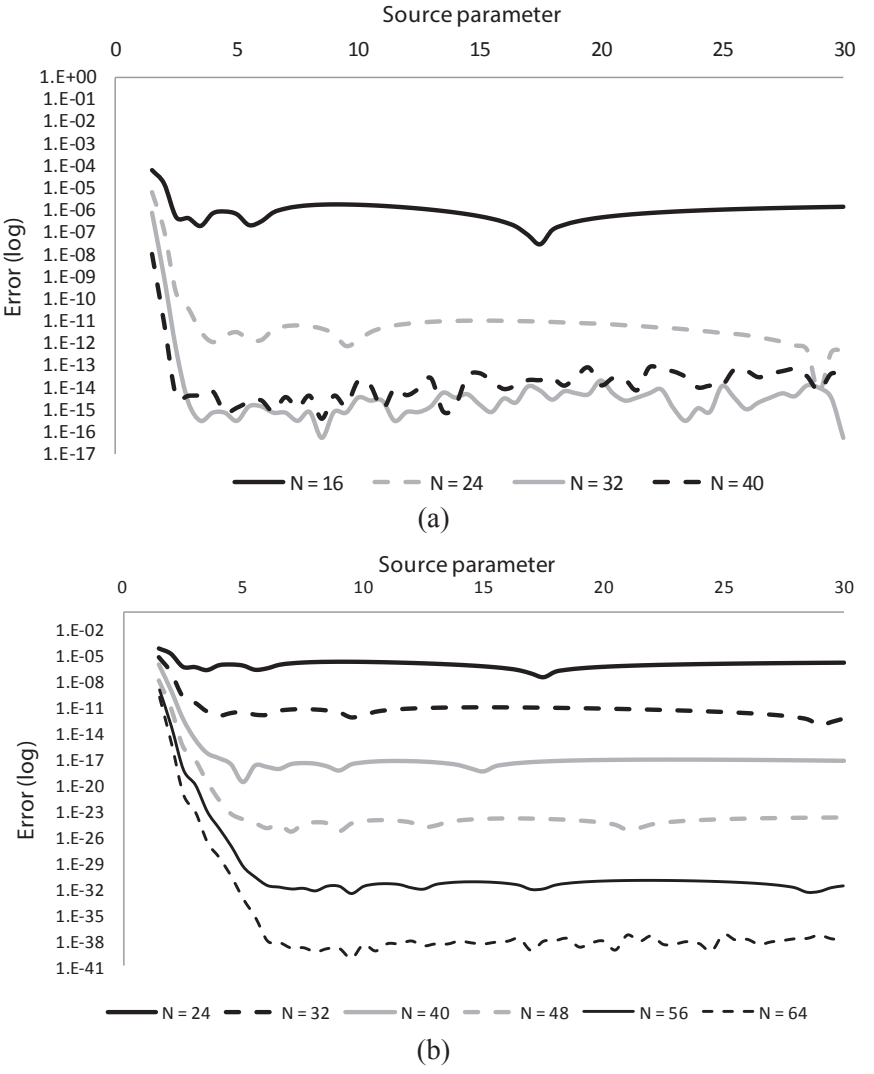

Figure 13: Relation between accuracy and source parameter for (a) IEEE extended precision and (b) MPFR ($p = 150$) for mode (o,1,1) eigenvalue in Example 2.

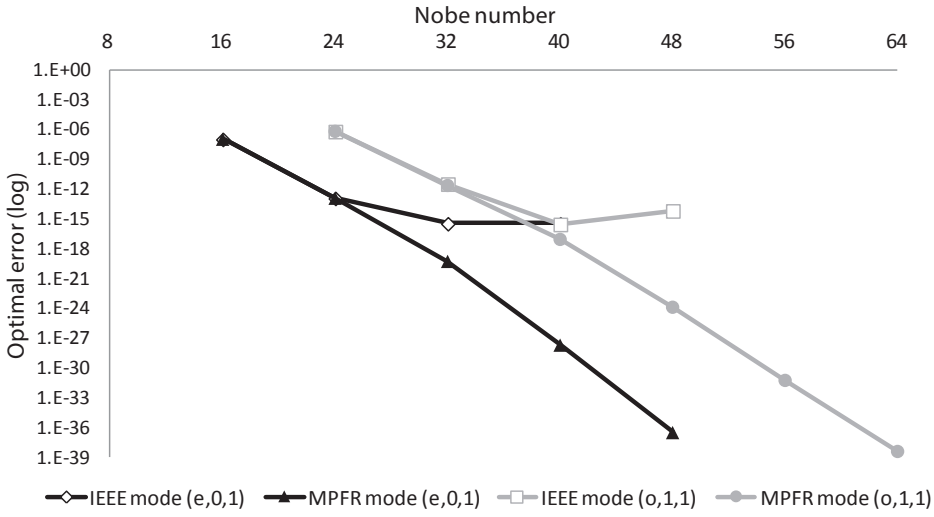

Figure 14: The exponential convergences of eigenvalues for different modes of Example 2.

Example 3:

Finally, we apply the proposed method to a doubly-connected Neumann problem. Consider the annular domain with inner radius $\rho_1 = 0.5$ and outer radius $\rho_2 = 2$. The problem is governed by the Helmholtz equation (1) and Neumann boundary condition (3). In this example, the polar coordinates (r, θ) are defined as

$$\begin{cases} x = r\cos\theta \\ y = r\sin\theta \end{cases} \tag{25}$$

where the radial coordinate r is a nonnegative real number and $0 \leq \theta < 2\pi$ is an angular coordinate. Obviously, we have the analytical eigenvalues given as the positive roots of

$$J'_m\left(k'r_2\right)Y'_m\left(k'r_1\right) - J'_m\left(k'r_1\right)Y'_m\left(k'r_2\right) = 0 \tag{26}$$

and the corresponding eigenfunctions are

$$\left\{J_m\left(k'r\right)Y'_m\left(k'r_1\right) - J'_m\left(k'r_1\right)Y_m\left(k'r\right)\right\}\left\{C_1\cos m\theta + C_2\sin m\theta\right\} \tag{27}$$

where C_1 and C_2 are normalization constants and m is a nonnegative integer. In Eqs. (26) and (27), J_m and Y_m are Bessel functions of order m.

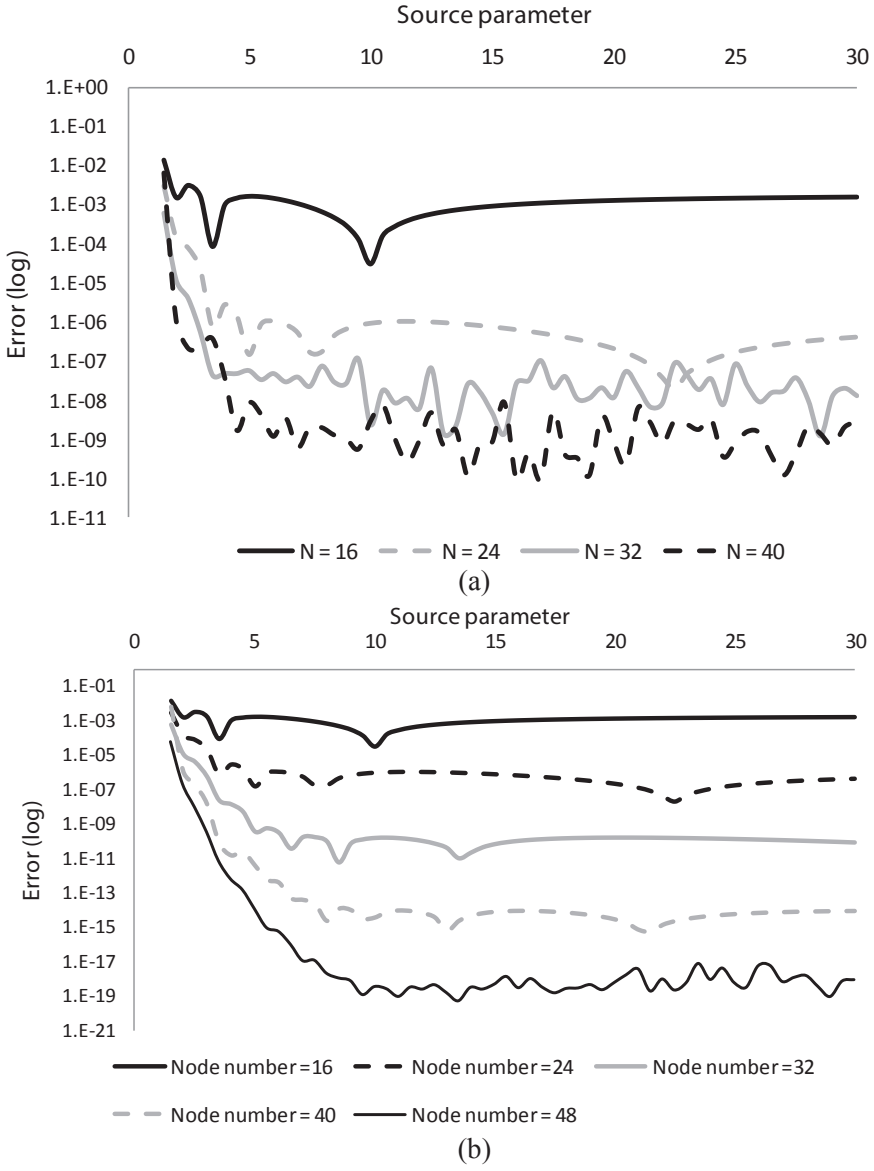

Figure 15: Relation between accuracy and source parameter for (a) IEEE extended precision and (b) MPFR ($p = 150$) for mode (e,0,1) eigenfunction in Example 2.

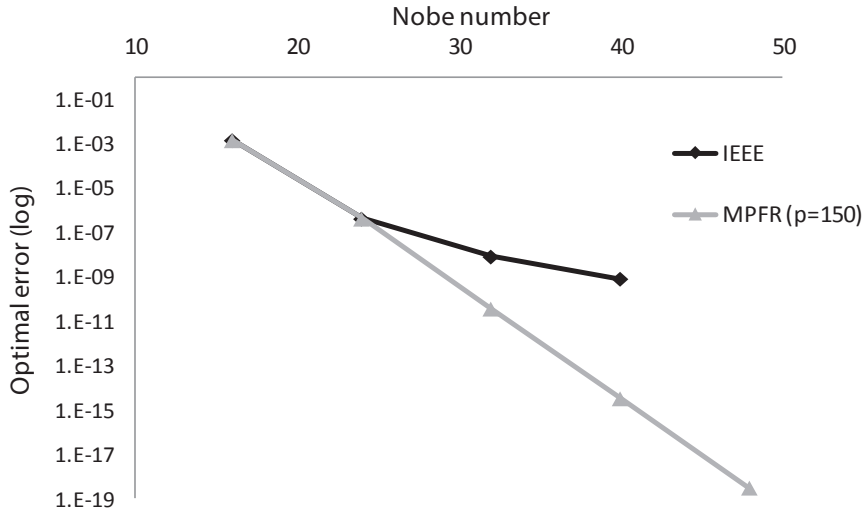

Figure 16: The exponential convergence of mode (e,0,1) eigenfunctions in Example 1.

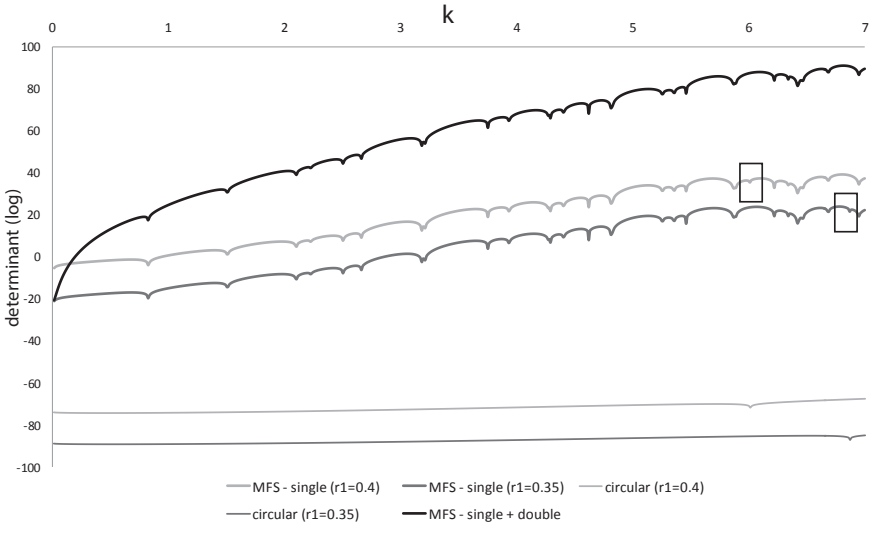

Figure 17: Results of UDSM of Example 3.

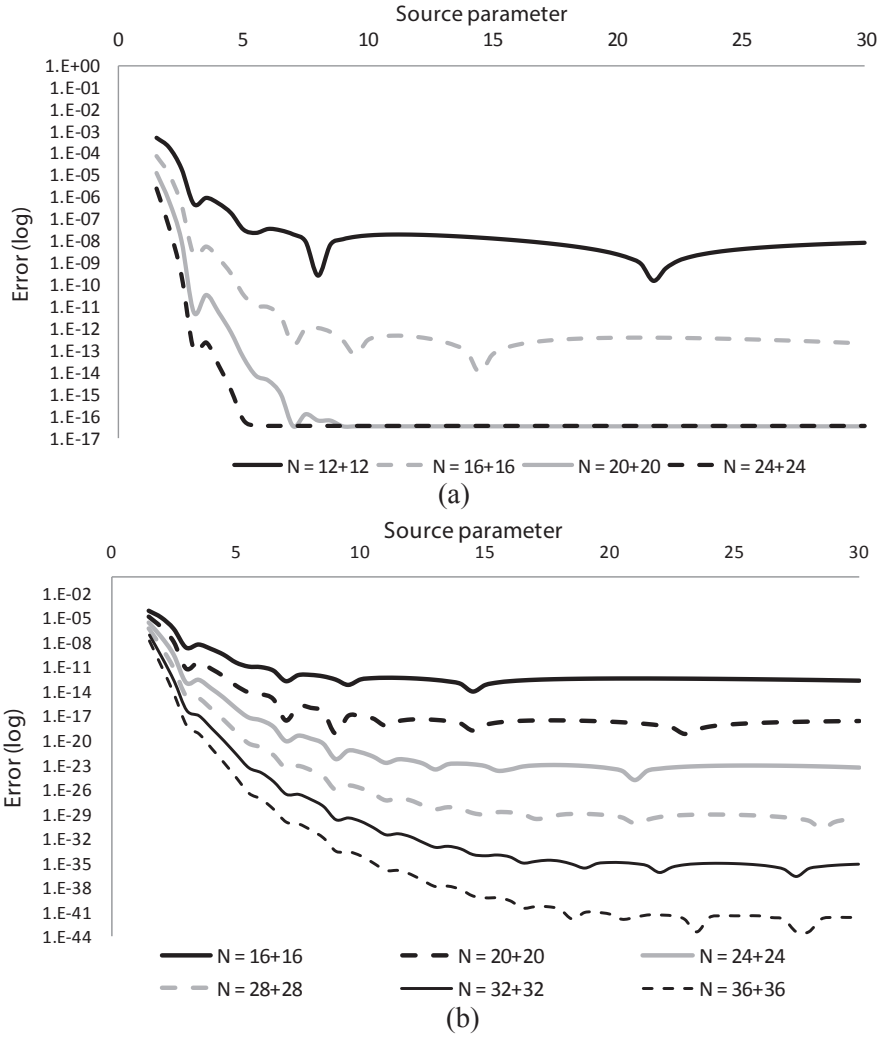

Figure 18: Relation between accuracy and source parameter for (a) IEEE extended precision and (b) MPFR ($p = 150$) for the eigenvalue in Example 3.

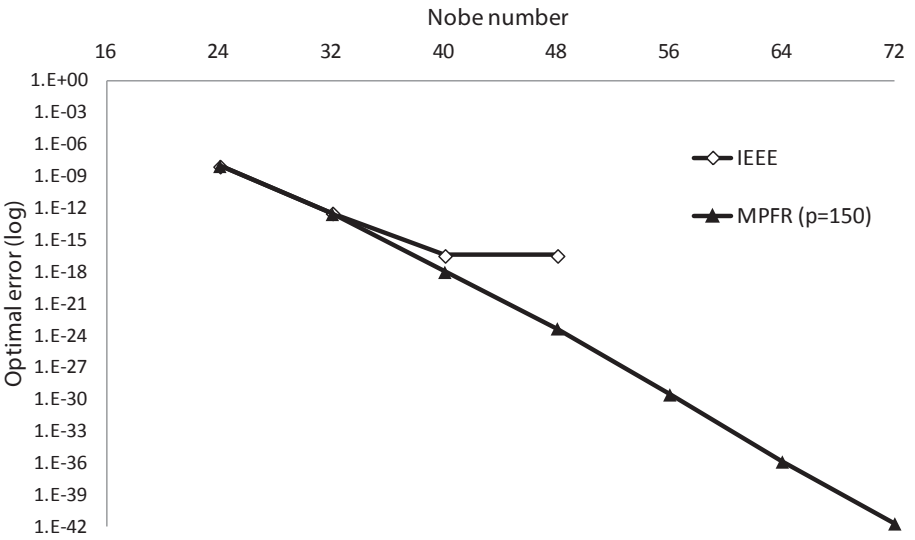

Figure 19: The exponential convergence of the eigenvalue in Example 3.

First, the UDSM is apply for both the single-layer MFS (6) and the mixed-layers MFS (10). In the numerical solutions, 32 outer sources are located on a circle with radius $r_2 = 3$ and 32 inner sources are located on a circle with radius $r_1 = 0.35$ or $r_1 = 0.4$ as shown in Figure 17. In the figure, it is clear that the single-layer MFS possesses spurious eigenvalues defined by a Dirichlet Helmholtz problem (1) & (2) with Γ^D being the curve of the interior sources ($r_1 = 0.35$ or $r_1 = 0.4$)

Then, the accuracy-source relations for the GSDSM eigenvalues and the least-squares MFS eigenfunctions for the smallest mode of Eq. (26) with $m = 1$ are given in Figures 18 and 20, respectively. In Figure 18 and 20, the source parameter is defined such that

$$\begin{cases} r_2 = \beta \rho_2 \\ r_1 = \dfrac{\rho_1}{\beta} \end{cases} \tag{28}$$

Then, their exponential convergences are given in Figures 19 and 21, respectively. These demonstrate the exponential convergence for the mixed-layers MFS (10) when it is applied for multiply-connected problems.

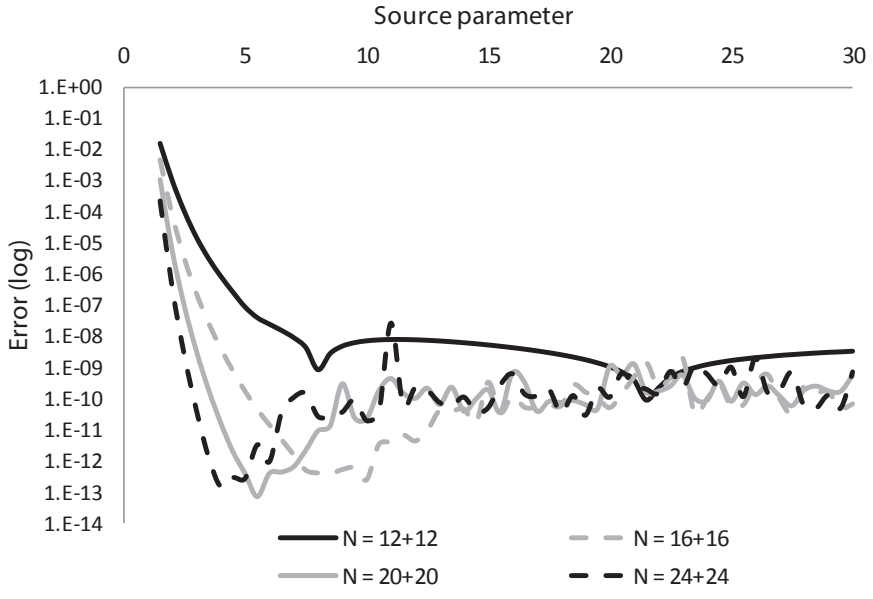

(a)

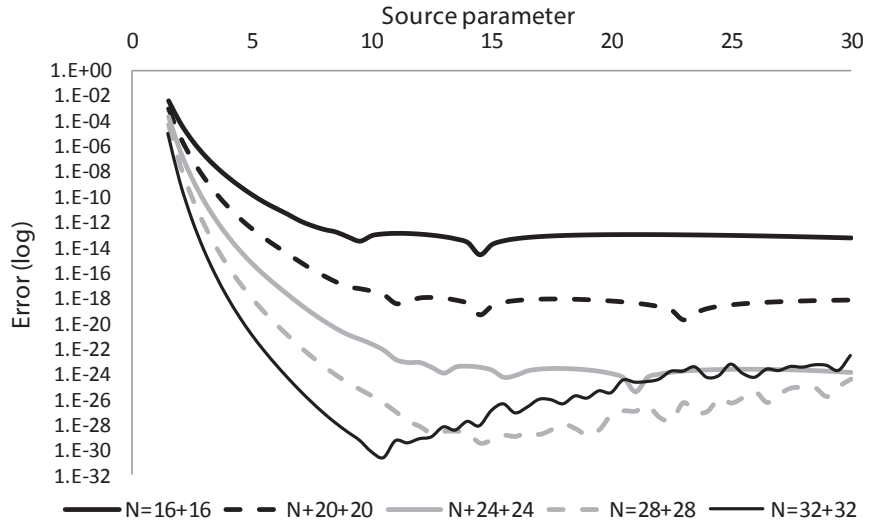

(b)

Figure 20: Relation between accuracy and source parameter for (a) IEEE extended precision and (b) MPFR ($p = 150$) for the eigenfunction in Example 3:

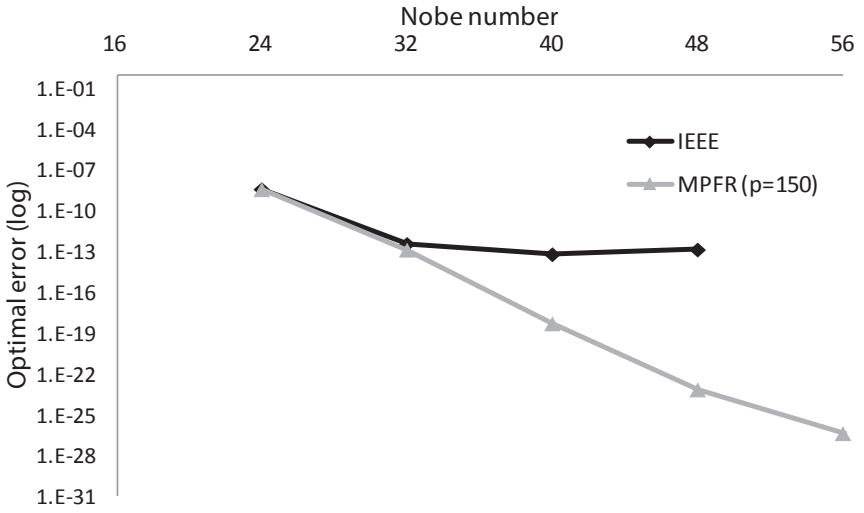

Figure 21: The exponential convergence of the eigenfunction in Example 3.

6 Conclusion

The exponential convergences of the method of fundamental solutions (MFS) for solving Helmholtz eigenvalues and eigenfunctions were demonstrated. In other words, the logarithmic value of optimal accuracy is proportional to number of boundary nodes. For eigenvalues, a golden section determinant search method (GSDSM) was developed for obtaining accurate eigenvalues with few iteration steps. The phenomenon of precision saturation was defined such that increasing resolution cannot improve the accuracy without increasing precision. By using the multiple precision floating-point reliable (MPFR) library, the MFS sources were located even farther and the solution accuracy could be further improved. For example, using the GSDSM with 48 nodes we obtained a numerical eigenvalue with accuracy up to 2.99×10^{-37} by simply put the sources to a eleven times bigger ellipse. In addition, the exponential convergence of the eigenfunctions obtained by the least-squares method of fundamental solutions was also demonstrated.

Acknowledgement: The National Science Council of Taiwan under NSC 101-2628- E-022-001-MY2 are gratefully acknowledged for providing financial support to carry out the present work.

References

Alhargan, F. A. (2000a): Algorithm 804: subroutines for the computation of Mathieu functions of integer orders. *ACM Trans. Math. Softw.*, vol. 26, pp. 408-414.

Alhargan, F. A. (2000b): Algorithms for the computation of all Mathieu functions of integer orders. *ACM Trans. Math. Softw.*, vol. 26, pp. 390-407.

Alves, C. J. S.; Silvestre, A. L. (2004): Density results using Stokeslets and a method of fundamental solutions for the Stokes equations. *Engineering Analysis with Boundary Elements*, vol. 28, pp. 1245-1252.

Bailey, D. H.; Borwein, J. M. (2008): *High-precision computation and mathematical physics*. XII Advanced Computing and Analysis Techniques in Physics Research, Italy, Proceeding of Science.

Bailey, D. H.; Yozo, H.; Li, X. S.; Thompson, B. (2002): "ARPREC: An arbitrary precision computation package." from http://crd.lbl.gov/∼dhbailey/dhbpapers/arprec.pdf.

Batut, C.; Belabas, K.; Bernardi, D.; Cohen, H.; Oliver, M. (2000): "PARI/GP." from http://pari.math.u-bordeaux.fr/.

Bogomolny, A. (1985): Fundamental solutions method for elliptic boundary value problems. *SIAM Journal on Numerical Analysis*, vol. 22, pp. 644-669.

Brent, R. P. (1978): A Fortran Multiple-Precision Arithmetic Package. *ACM Trans. Math. Softw.*, vol. 4, pp. 57-70.

Char, B. W.; Geddes, K. O.; Gonnet, G. H.; Leong, B. L.; Monagan, M. B.; Watt, S. M. (1991): *Maple V: language reference manual*, Springer-Verlag.

Chen, C. S.; Cho, H. A.; Golberg, M. A. (2006): Some comments on the ill-conditioning of the method of fundamental solutions. *Engineering Analysis with Boundary Elements*, vol. 30, pp. 405-410.

Chen, C. W.; Young, D. L.; Tsai, C. C.; Murugesan, K. (2005): The method of fundamental solutions for inverse 2D Stokes problems. *Computational Mechanics*, vol. 37, pp. 2-14.

Chen, J. T.; Chen, I. L.; Lee, Y. T. (2005): Eigensolutions of multiply connected membranes using the method of fundamental solutions. *Engineering Analysis with Boundary Elements*, vol. 29, pp. 166-174.

Chen, J. T.; Chen, K. H.; Chyuan, S. W. (1999): Numerical experiments for acoustic modes of a square cavity using the dual boundary element method. *Applied Acoustics*, vol. 57, pp. 293-325.

Chen, J. T.; Huang, C. X.; Wong, F. C. (2000): Determination of spurious eigenvalues and multiplicities of true eigenvalues in the dual multiple reciprocity method

using the singular-value decomposition technique. *Journal of Sound and Vibration*, vol. 230, pp. 203-219.

Christiansen, S.; Meister, E. (1981): Condition number of matrices derived from two classes of integral equations. *Mathematical Methods in the Applied Sciences*, vol. 3, pp. 364-392.

Fairweather, G.; Karageorghis, A. (1998): The method of fundamental solutions for elliptic boundary value problems. *Advances in Computational Mathematics*, vol. 9, pp. 69-95.

Fousse, L.; Hanrot, G.; Lefevre, V.; Pelissier, P.; Zimmermann, P. (2007): MPFR: A multiple-precision binary floating-point library with correct rounding. *ACM Trans. Math. Softw.*, vol. 33, pp. 13.

Frank, W. O.; Daniel, W. L.; Ronald, F. B.; Charles, W. C. (2010): *NIST Handbook of Mathematical Functions*, Cambridge University Press.

Golberg, M. A. (1995): The method of fundamental solutions for Poisson's equation. *Engineering Analysis with Boundary Elements*, vol. 16, pp. 205-213.

Golberg, M. A.; Chen, C. S., Eds. (1999): *The method of fundamental solutions for potential, Helmholtz and diffusion problems*. Boundary Integral Methods: Numerical and Mathematical Aspects. Southampton, Computational Mechanics Publications.

Granlund, T. (2004): "GMP: the GNU multiple precision arithmetic library." from http://gmplib.org/.

Gu, M. H.; Young, D. L.; Fan, C. M. (2009): The method of fundamental solutions for one-dimensional wave equations. *Computers, Materials & Continua (CMC)*, vol. 11, pp. 185-208.

Haible, B.; Kreckel, R. (2005): "CLN, class library for numbers.", from http://www.ginac.de/CLN/.

Hanrot, G.; Lefevre, V.; Pelissier, P.; Zimmermann, P. (2005): "The GNU MPFR library." from http://www.mpfr.org/.

Johnston, R. L.; Fairweather, G. (1984): The method of fundamental solutions for problems in potential flow. *Applied Mathematical Modelling*, vol. 8, pp. 265-270.

Karageorghis, A. (2001): The method of fundamental solutions for the calculation of the eigenvalues of the Helmholtz equation. *Applied Mathematics Letters*, vol. 14, pp. 837-842.

Karageorghis, A.; Fairweather, G. (1987): The method of fundamental solutions for the numerical solution of the biharmonic equation. *Journal of Computational Physics*, vol. 69, pp. 434-459.

Kondapalli, P. S.; Shippy, D. J.; Fairweather, G. (1992): Analysis of acoustic scattering in fluids and solids by the method of fundamental solutions. *The Journal of the Acoustical Society of America*, vol. 91, pp. 1844-1854.

Kupradze, V. D.; Aleksidze, M. A. (1964): The method of functional equations for the approximate solution of certain boundary value problems. *USSR Computational Mathematics and Mathematical Physics*, vol. 4, pp. 82-126.

Lin, C. Y.; Gu, M. H.; Young, D. L. (2010): The time-marching method of fundamental solutions for multi-dimensional telegraph equations. *Computers, Materials & Continua (CMC)*, vol. 18, pp. 43.

Mathon, R.; Johnston, R. L. (1977): The approximate solution of elliptic boundary-value problems by fundamental solutions. *SIAM Journal on Numerical Analysis*, vol. 14, pp. 638-650.

Ramachandran, P. A. (2002): Method of fundamental solutions: singular value decomposition analysis. *Communications in Numerical Methods in Engineering*, vol. 18, pp. 789-801.

Santos, W. J.; Santiago, J. A. F.; Telles, J. C. F. (2012): An Application of Genetic Algorithms and the Method of Fundamental Solutions to Simulate Cathodic Protection Systems. *Computer Modeling in Engineering & Sciences(CMES)*, vol. 87, pp. 23-40.

Smyrlis, Y. S.; Karageorghis, A. (2004): A linear least-squares MFS for certain elliptic problems. *Numerical Algorithms*, vol. 35, pp. 29-44.

Smyrlis, Y. S.; Karageorghis, A.; Georgiou, G. (2001): Some aspects of the one-dimensional version of the method of fundamental solutions. *Computers & Mathematics with Applications*, vol. 41, pp. 647-657.

Tsai, C. C.; Lin, P. H. (2013): On the exponential convergence of the method of fundamental solutions. *International Journal of Computational Methods*, vol. 10, pp. 1341007.

Tsai, C. C. (2007): The method of fundamental solutions for three-dimensional elastostatic problems of transversely isotropic solids. *Engineering Analysis with Boundary Elements*, vol. 31, pp. 586-594.

Tsai, C. C. (2009): The method of fundamental solutions with dual reciprocity for three-dimensional thermoelasticity under arbitrary body forces. *Engineering Computations*, vol. 26, pp. 229-244.

Tsai, C. C.; Lin, Y. C.; Young, D. L.; Aturi, S. N. (2006): Investigations on the accuracy and condition number for the method of fundamental solutions. *CMES: Computer Modeling in Engineering & Sciences*, vol. 16, pp. 103-114.

Tsai, C. C.; Young, D. L.; Chen, C. W.; Fan, C. M. (2006): The method of fun-

damental solutions for eigenproblems in domains with and without interior holes. *Proceedings of the Royal Society A-Mathematical Physical and Engineering Sciences*, vol. 462, pp. 1443-1466.

Tsai, C. C.; Young, D. L.; Chiu, C. L.; Fan, C. M. (2009): Numerical analysis of acoustic modes using the linear least squares method of fundamental solutions. *Journal of Sound and Vibration*, vol. 324, pp. 1086-1110.

Tsai, C. C.; Young, D. L.; Fan, C. M.; Chen, C. W. (2006): MFS with time-dependent fundamental solutions for unsteady Stokes equations. *Engineering Analysis with Boundary Elements*, vol. 30, pp. 897-908.

Tsai, C. C.; Young, D. L.; Lo, D. C.; Wong, T. K. (2006): Method of fundamental solutions for three-dimensional stokes flow in exterior field. *Journal of Engineering Mechanics-Asce*, vol. 132, pp. 317-326.

Wei, T.; Hon, Y. C.; Ling, L. (2007): Method of fundamental solutions with regularization techniques for Cauchy problems of elliptic operators. *Engineering Analysis with Boundary Elements*, vol. 31, pp. 373-385.

William, H.; Teukolsky, S. A. (1988): *Numerical Recipes in C: The art of scientific computing*, Cambridge university press.

Wolfram, S. (1996): *The Mathematica book*, Cambridge University Press.

Wu, C. T.; Yang, F. L.; Young, D. L. (2011): Application of the method of fundamental solutions and the generalized Lagally theorem to the interaction of solid body and external singularities in an inviscid fluid. *Computers Materials and Continua (CMC)*, vol. 23, pp. 135.

Young, D. L.; Jane, S. J.; Fan, C. M.; Murugesan, K.; Tsai, C. C. (2006): The method of fundamental solutions for 2D and 3D Stokes problems. *Journal of Computational Physics*, vol. 211, pp. 1-8.

Young, D. L.; Tsai, C. C.; Fan, C. M. (2004): Direct approach to solve nonhomogeneous diffusion problems using fundamental solutions and dual reciprocity methods. *Journal of the Chinese Institute of Engineers*, vol. 27, pp. 597-609.

Young, D. L.; Tsai, C. C.; Murugesan, K.; Fan, C. M.; Chen, C. W. (2004): Time-dependent fundamental solutions for homogeneous diffusion problems. *Engineering Analysis with Boundary Elements*, vol. 28, pp. 1463-1473.